# INTEREST JINR
## Wave 3

# Radiation Protection and the Safety of Radiation Sources

Project

08 February - 19 March, 2021

Prepared by:

**Alaa ElSadieque**

Research Fellow in Alexandria University Cancer Research Cluster

Egypt

Under Supervision of:

**Prof.Dr.Said AbouElazm**

# Task1

## BGO Detector:

$$\text{Resolution} = \frac{sigma * 2.35}{mean}$$

Sigma = FWHM

Mean =peak position

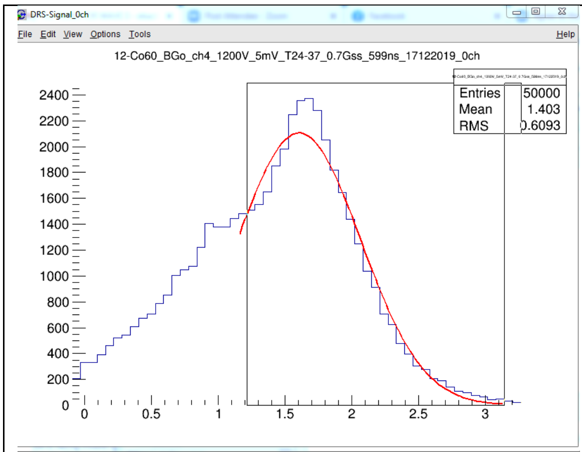

| | |
|---|---|
| Entries | 50000 |
| Mean | 1.403 |
| RMS | 0.6093 |

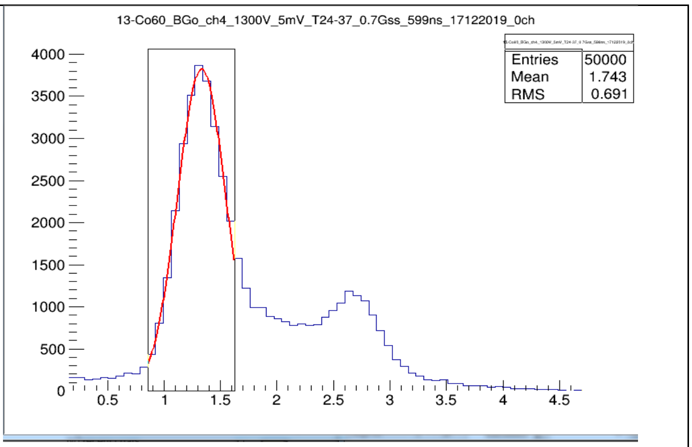

| | |
|---|---|
| Entries | 50000 |
| Mean | 1.743 |
| RMS | 0.691 |

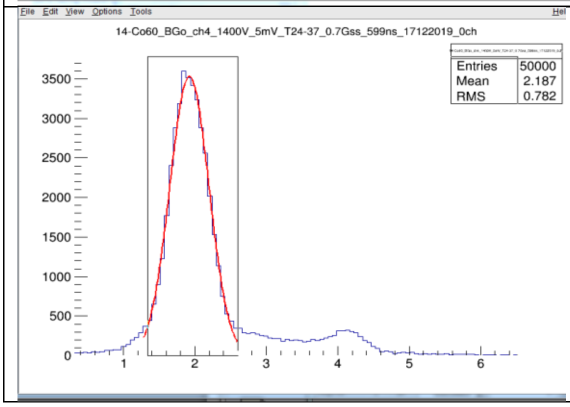

| | |
|---|---|
| Entries | 50000 |
| Mean | 2.187 |
| RMS | 0.782 |

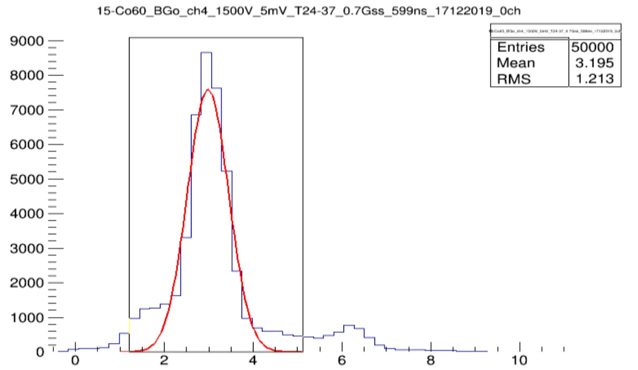

| | |
|---|---|
| Entries | 50000 |
| Mean | 3.195 |
| RMS | 1.213 |

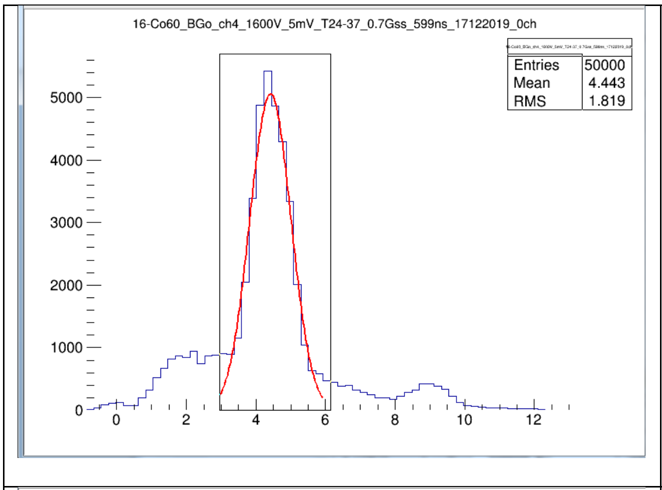
16-Co60_BGo_ch4_1600V_5mV_T24-37_0.7Gss_599ns_17122019_0ch
Entries 50000
Mean 4.443
RMS 1.819
0
1000
2000
3000
4000
5000
0
2
4
6
8
10
12

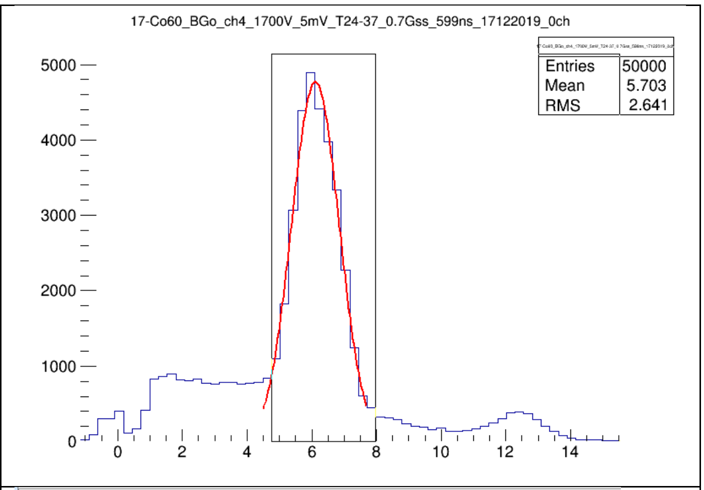
17-Co60_BGo_ch4_1700V_5mV_T24-37_0.7Gss_599ns_17122019_0ch
Entries 50000
Mean 5.703
RMS 2.641
0
1000
2000
3000
4000
5000
0
2
4
6
8
10
12
14

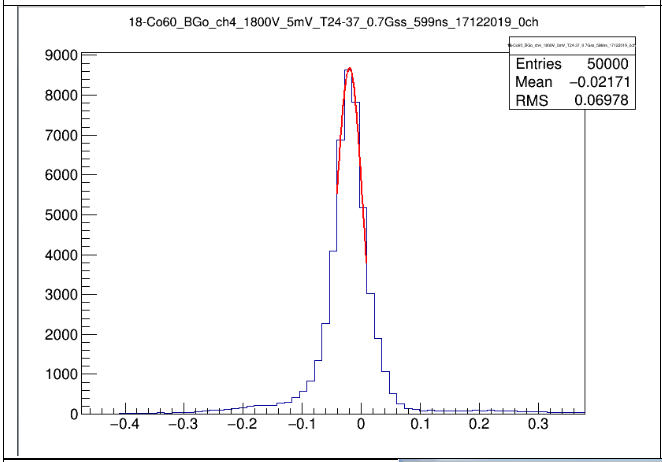
18-Co60_BGo_ch4_1800V_5mV_T24-37_0.7Gss_599ns_17122019_0ch
Entries 50000
Mean −0.02171
RMS 0.06978
0
1000
2000
3000
4000
5000
6000
7000
8000
9000
−0.4
−0.3
−0.2
−0.1
0
0.1
0.2
0.3

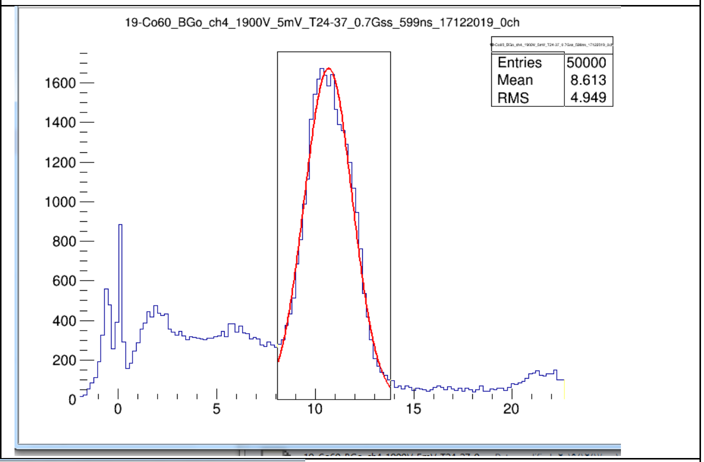
19-Co60_BGo_ch4_1900V_5mV_T24-37_0.7Gss_599ns_17122019_0ch
Entries 50000
Mean 8.613
RMS 4.949
0
200
400
600
800
1000
1200
1400
1600
0
5
10
15
20

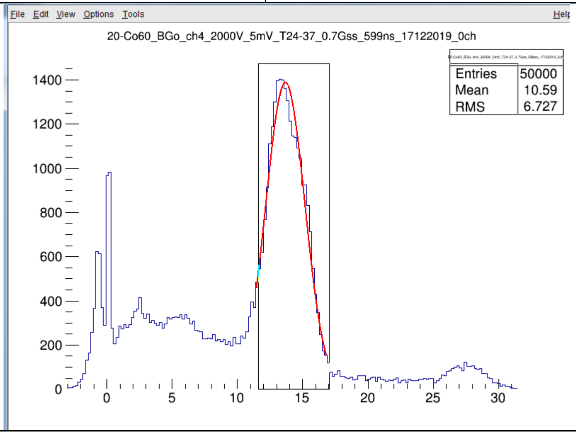
File
Edit
View
Options
Tools
Help
20-Co60_BGo_ch4_2000V_5mV_T24-37_0.7Gss_599ns_17122019_0ch
Entries 50000
Mean 10.59
RMS 6.727
0
200
400
600
800
1000
1200
1400
0
5
10
15
20
25
30

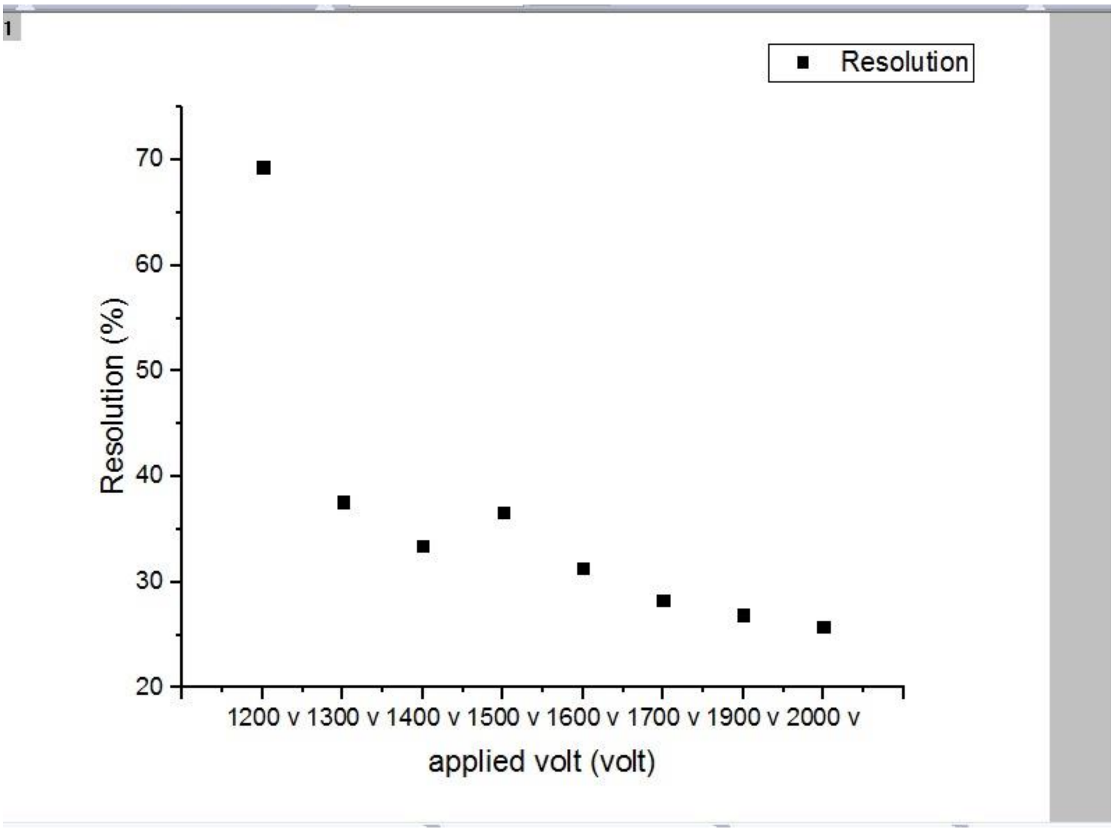

# NaI Detector:

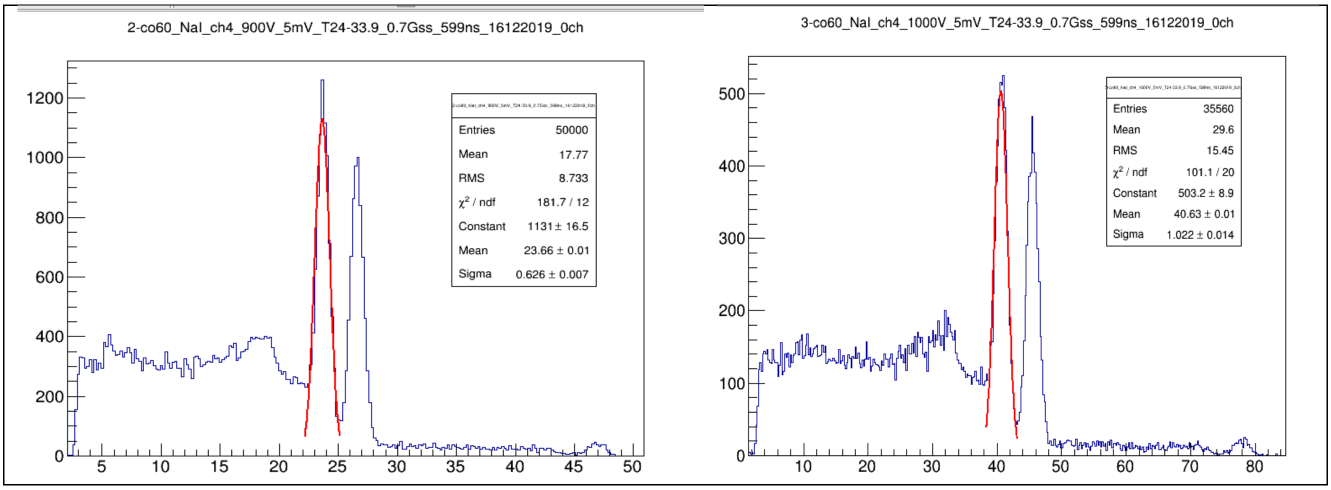

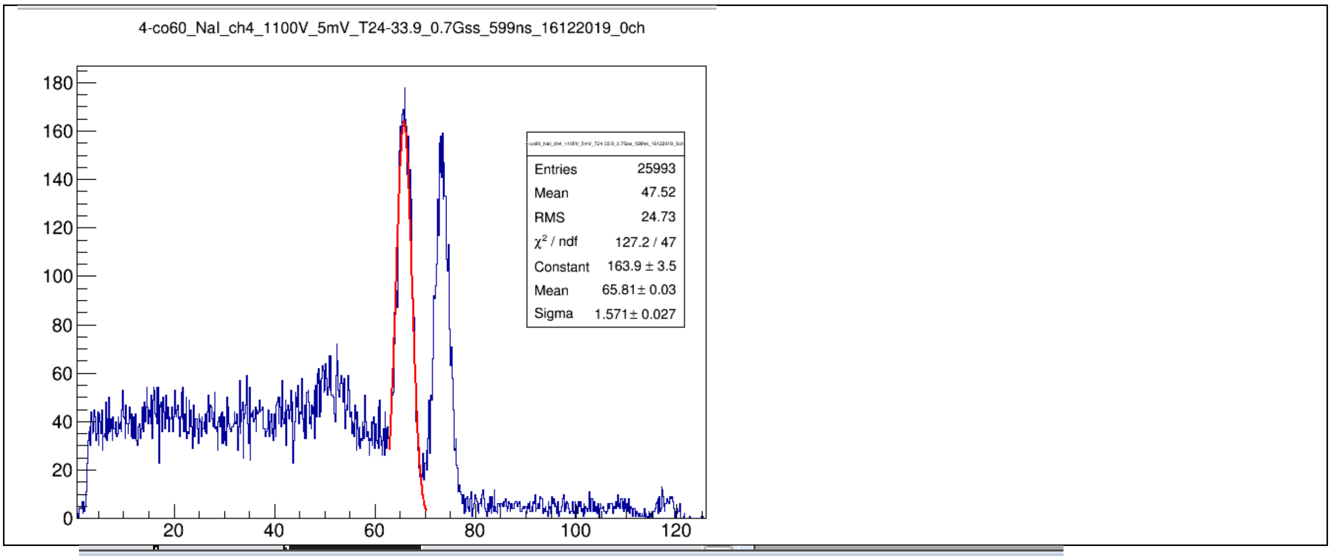
4-co60_NaI_ch4_1100V_5mV_T24-33.9_0.7Gss_599ns_16122019_0ch
Entries 25993
Mean 47.52
RMS 24.73
χ² / ndf 127.2 / 47
Constant 163.9 ± 3.5
Mean 65.81 ± 0.03
Sigma 1.571 ± 0.027
0
20
40
60
80
100
120
140
160
180
20
40
60
80
100
120

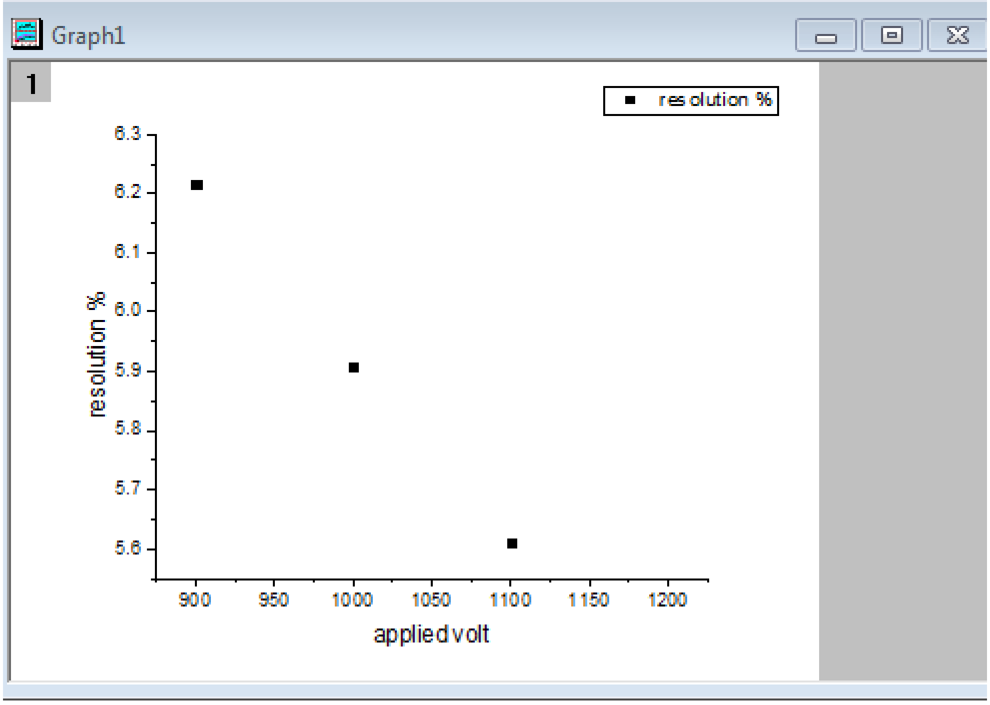
Graph1
1
resolution %
resolution %
6.3
6.2
6.1
6.0
5.9
5.8
5.7
5.6
900
950
1000
1050
1100
1150
1200
applied volt

# Task2

## BGO-Co60+Cs137-800v calibration

1. Fitting 4 highest peak
2. Set parameter
3. Determine (pmt= mean) & the energy in MeV
4. The energy of first peak (Cs$^{137}$) is 0.662 MeV
   Second peak (Co$^{60}$) is 1.17 MeV
   third peak (Co$^{60}$) is 1.17 MeV
5. The energy fourth peak (sum of two Co$^{60}$ specta) is 1.17 MeV

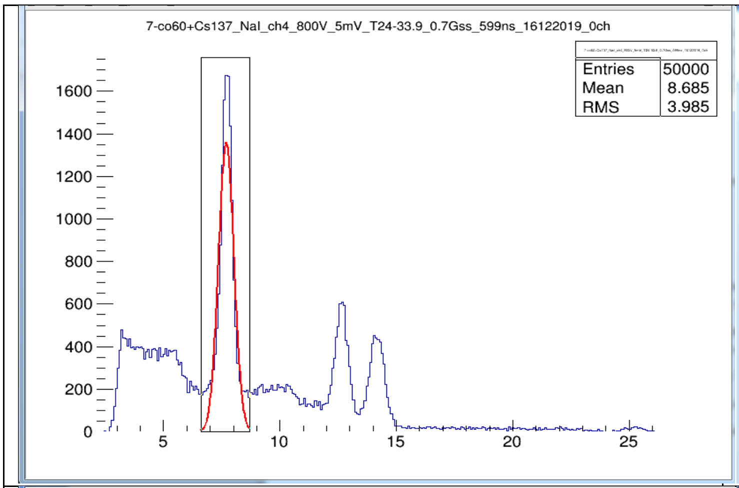

Entries 50000
Mean 8.685
RMS 3.985

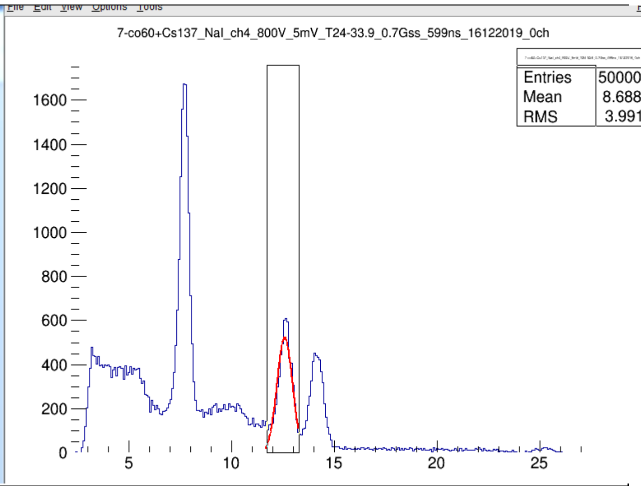

Entries 50000
Mean 8.688
RMS 3.991

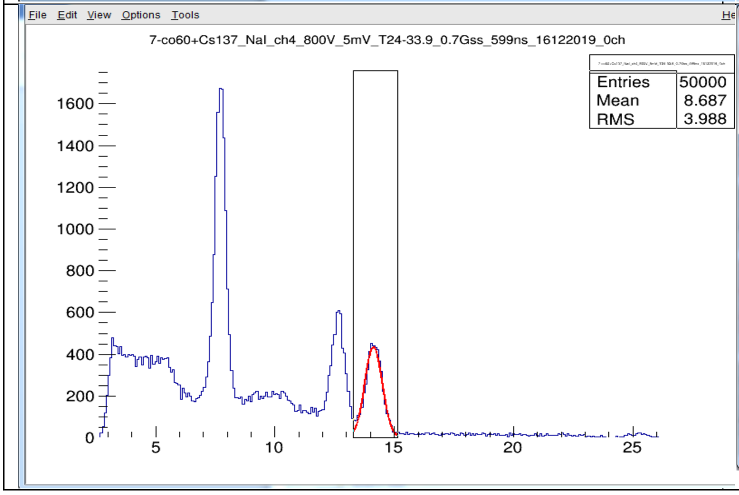

Entries 50000
Mean 8.687
RMS 3.988

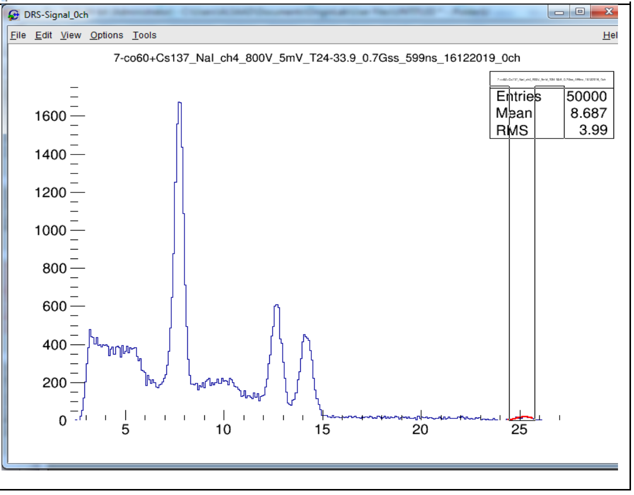

Entries 50000
Mean 8.687
RMS 3.99

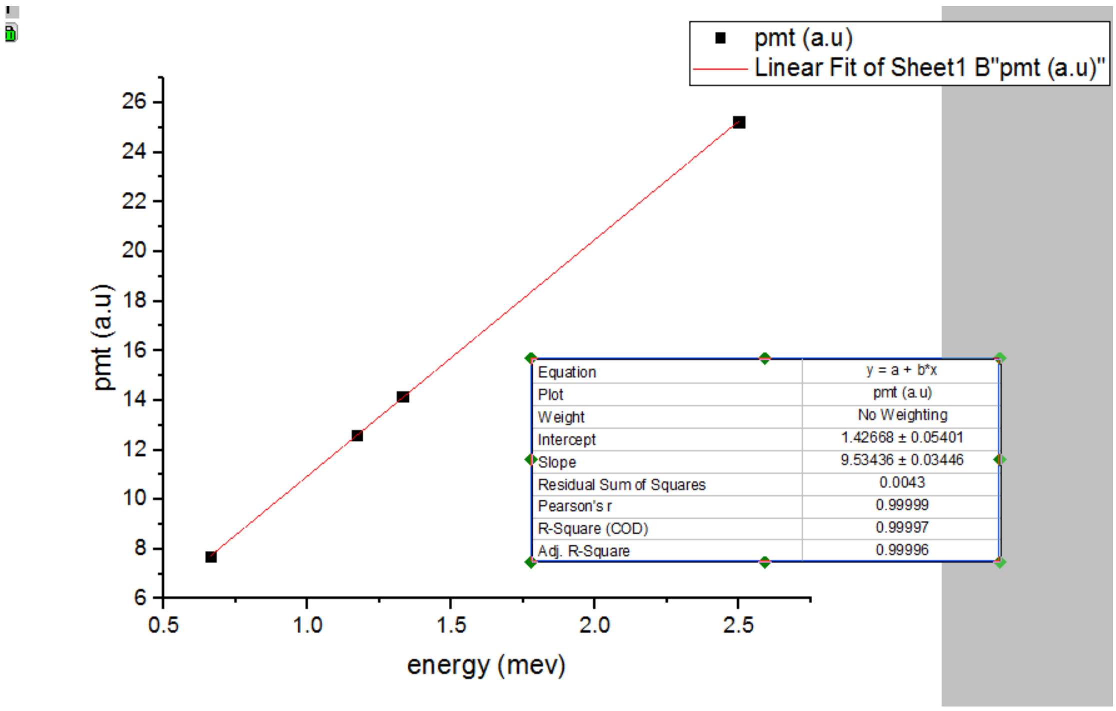

| | |
|---|---|
| Equation | y = a + b*x |
| Plot | pmt (a.u) |
| Weight | No Weighting |
| Intercept | 1.42668 ± 0.05401 |
| Slope | 9.53436 ± 0.03446 |
| Residual Sum of Squares | 0.0043 |
| Pearson's r | 0.99999 |
| R-Square (COD) | 0.99997 |
| Adj. R-Square | 0.99996 |

# Task 3

Unknown source1:

Mean= 6.288= y

$Y=bX+a$

The calibration form

$Y=9.53436X +1.42668$

$6.288= 9.53436\ X+1.42668$

$4.827= 9.50178X$

$X=0.5095=0.510$

E= 0.510 Mev

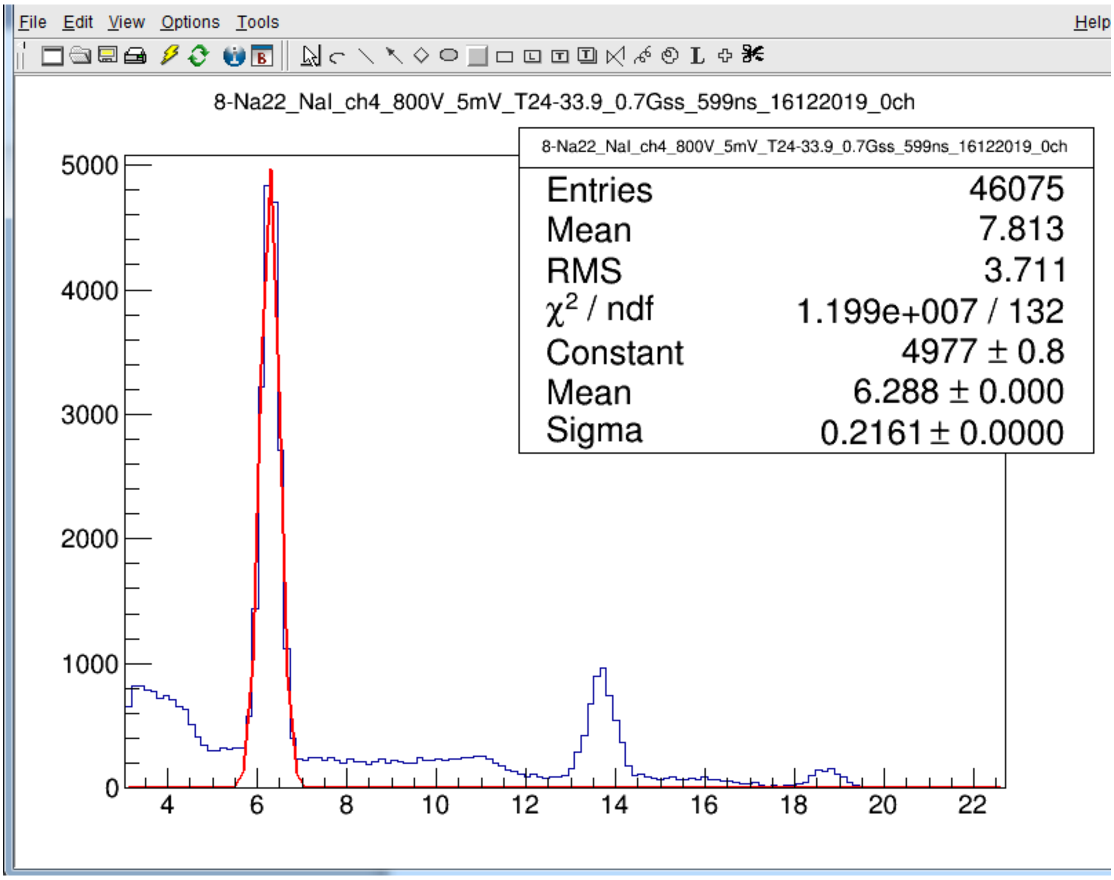

8-Na22_NaI_ch4_800V_5mV_T24-33.9_0.7Gss_599ns_16122019_0ch

| 8-Na22_NaI_ch4_800V_5mV_T24-33.9_0.7Gss_599ns_16122019_0ch | |
|---|---|
| Entries | 46075 |
| Mean | 7.813 |
| RMS | 3.711 |
| $\chi^2$ / ndf | 1.199e+007 / 132 |
| Constant | 4977 ± 0.8 |
| Mean | 6.288 ± 0.000 |
| Sigma | 0.2161 ± 0.0000 |

---

Unknown source2:

Mean= 4.66856

Y=9.53436X +1.42668

4.66856= 9.53436X +1.42668

X=0.340 Mev

Energy= 0.340 Mev

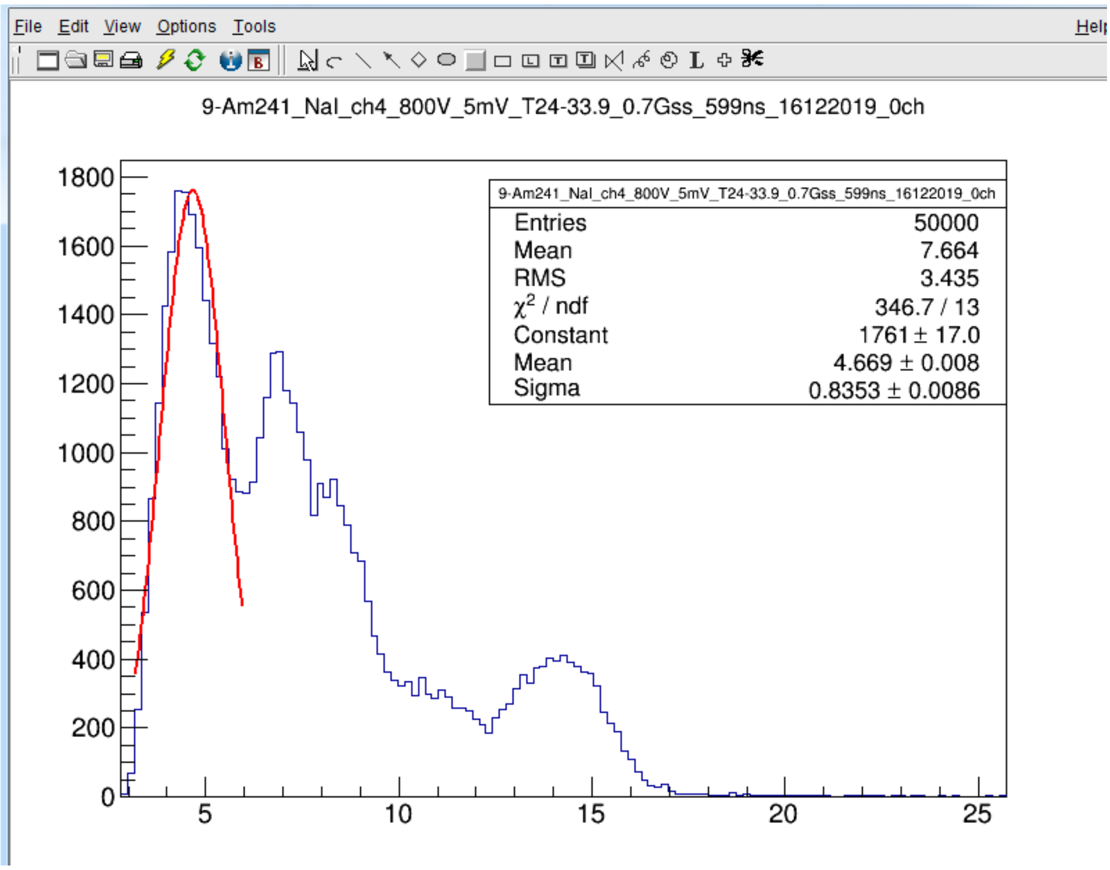

9-Am241_NaI_ch4_800V_5mV_T24-33.9_0.7Gss_599ns_16122019_0ch

| | |
|---|---|
| Entries | 50000 |
| Mean | 7.664 |
| RMS | 3.435 |
| $\chi^2$ / ndf | 346.7 / 13 |
| Constant | 1761 ± 17.0 |
| Mean | 4.669 ± 0.008 |
| Sigma | 0.8353 ± 0.0086 |

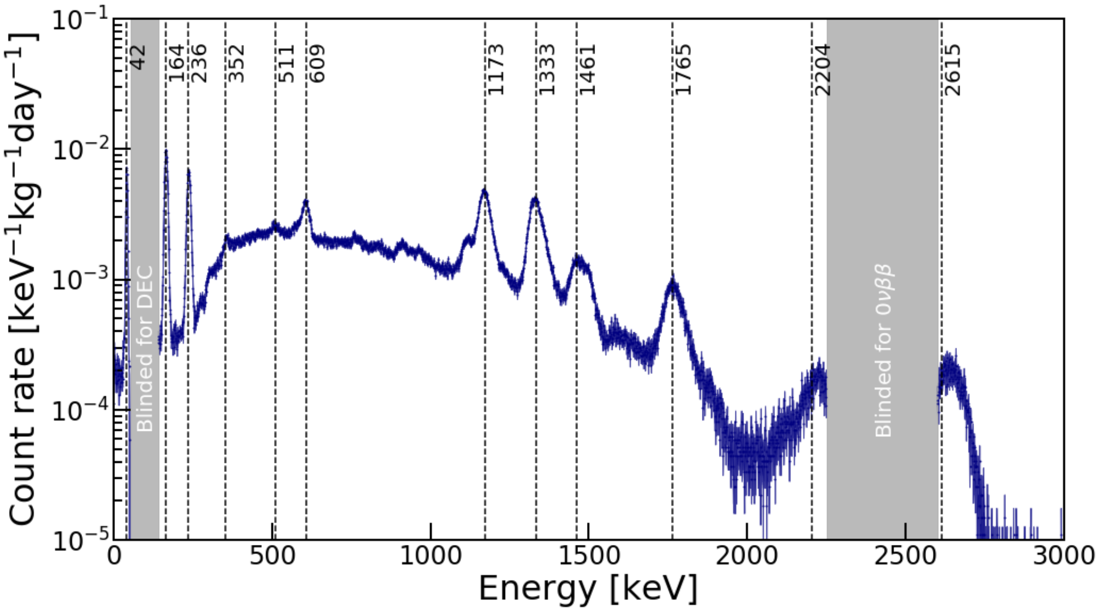
Count rate [keV$^{-1}$kg$^{-1}$day$^{-1}$]
$10^{-1}$
$10^{-2}$
$10^{-3}$
$10^{-4}$
$10^{-5}$
Energy [keV]
0
500
1000
1500
2000
2500
3000
42
164
236
352
511
609
1173
1333
1461
1765
2204
2615
Blinded for DEC
Blinded for $0\nu\beta\beta$

# Task 4

1. From attenuation equation

$I = I_0 e^{-\mu x}$

$I = I_0 e^{-\mu x}$

For Al material:

$I / I_0 = e^{-\mu x}$

| Thickness, cm | $I / I_0$ |
|---|---|
| 0 | 1 |
| 0.15 | 0.75573 |
| 0.3 | 0.71623 |
| 0.45 | 0.70569 |
| 0.75 | 0.68596 |
| 0.9 | 0.67155 |
| 1.08 | 0.66103 |
| 1.26 | 0.63939 |

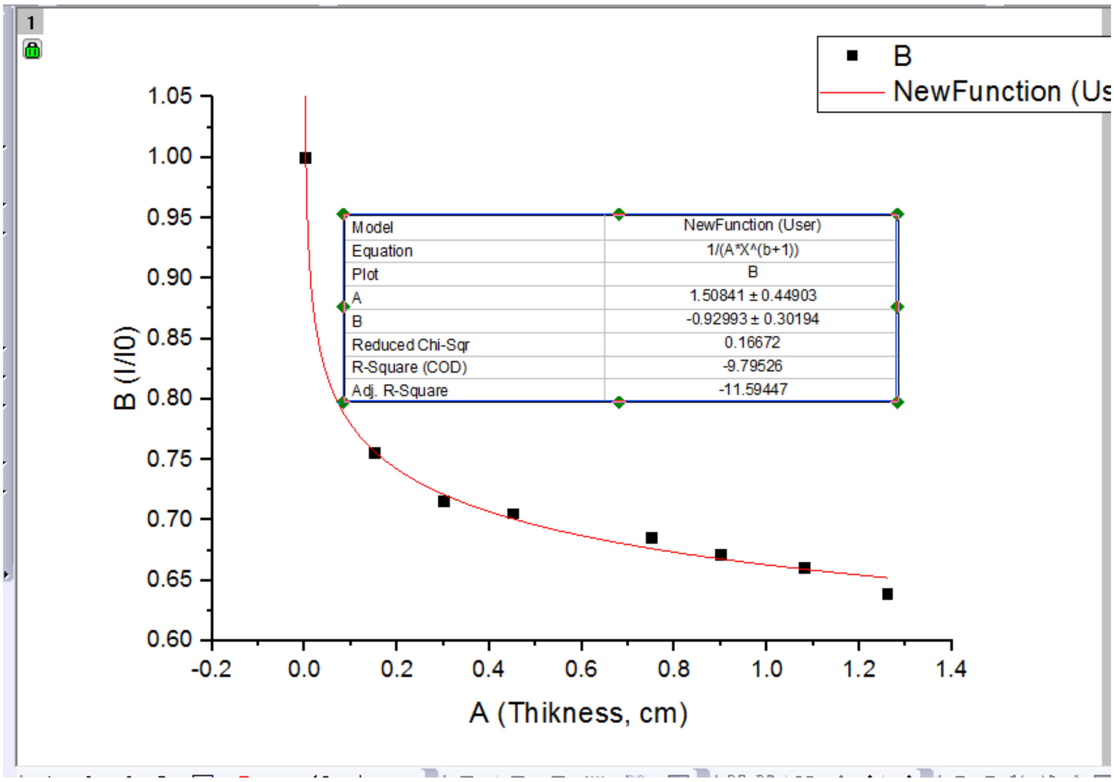

| | |
|---|---|
| Model | NewFunction (User) |
| Equation | 1/(A*X^(b+1)) |
| Plot | B |
| A | 1.50841 ± 0.44903 |
| B | -0.92993 ± 0.30194 |
| Reduced Chi-Sqr | 0.16672 |
| R-Square (COD) | -9.79526 |
| Adj. R-Square | -11.59447 |

$\mu$=0.93 cm$^{-1}$

---

For Cu material:

$$I = I_0 e^{-\mu x}$$

| Thickness, cm | $I / I_0$ |
|---|---|
| 0 | 1 |
| 0.2 | 0.75573 |
| 0.25 | 0.7357 |
| 0.4 | 0.68065 |
| 0.8 | 0.68065 |
| 1 | 0.53827 |
| 1.2 | 0.48042 |

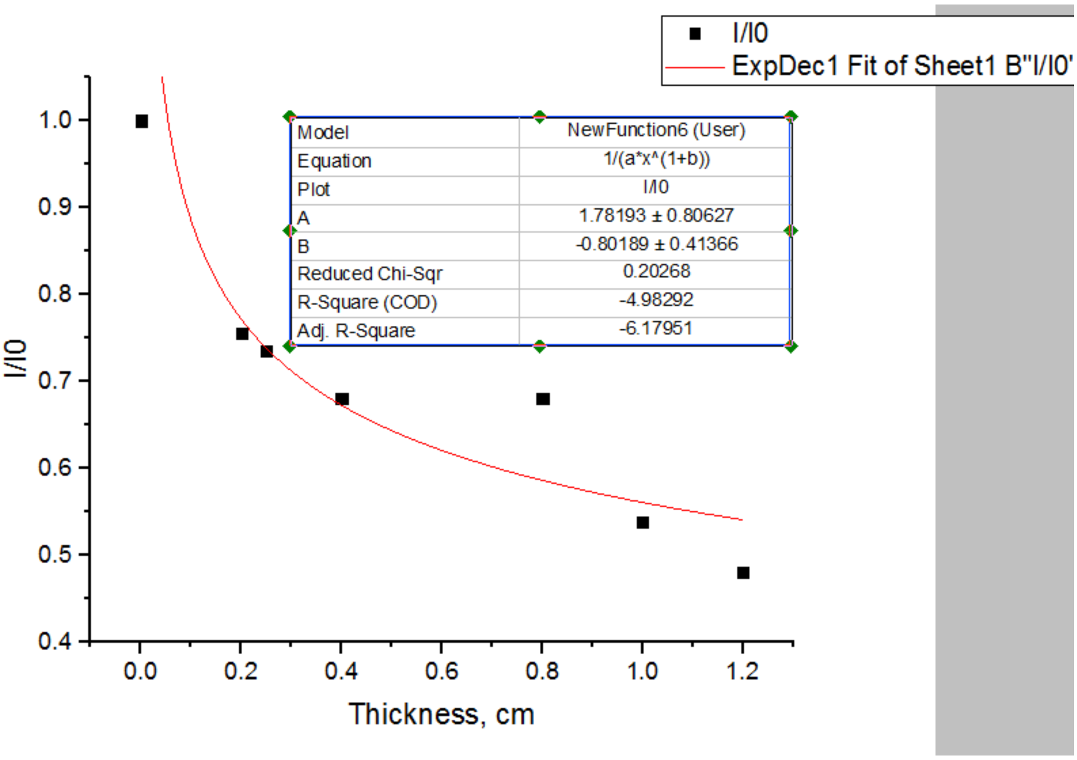

| | |
|---|---|
| Model | NewFunction6 (User) |
| Equation | 1/(a*x^(1+b)) |
| Plot | I/I0 |
| A | 1.78193 ± 0.80627 |
| B | -0.80189 ± 0.41366 |
| Reduced Chi-Sqr | 0.20268 |
| R-Square (COD) | -4.98292 |
| Adj. R-Square | -6.17951 |

$\mu$=0.8 cm$^{-1}$

# Task 5

There is a distance where none alpha particles are registered with the detector. This distance is the range of alpha particles in the air.According to graph the detector did not record any new reading in 3.5 Cm

$\therefore R = 3.5 \text{ cm}$

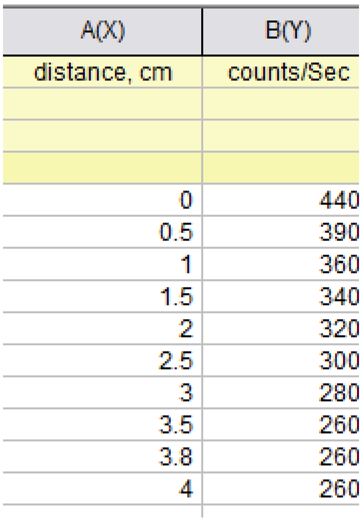

| A(X) | B(Y) |
|---|---|
| distance, cm | counts/Sec |
| | |
| | |
| | |
| 0 | 440 |
| 0.5 | 390 |
| 1 | 360 |
| 1.5 | 340 |
| 2 | 320 |
| 2.5 | 300 |
| 3 | 280 |
| 3.5 | 260 |
| 3.8 | 260 |
| 4 | 260 |

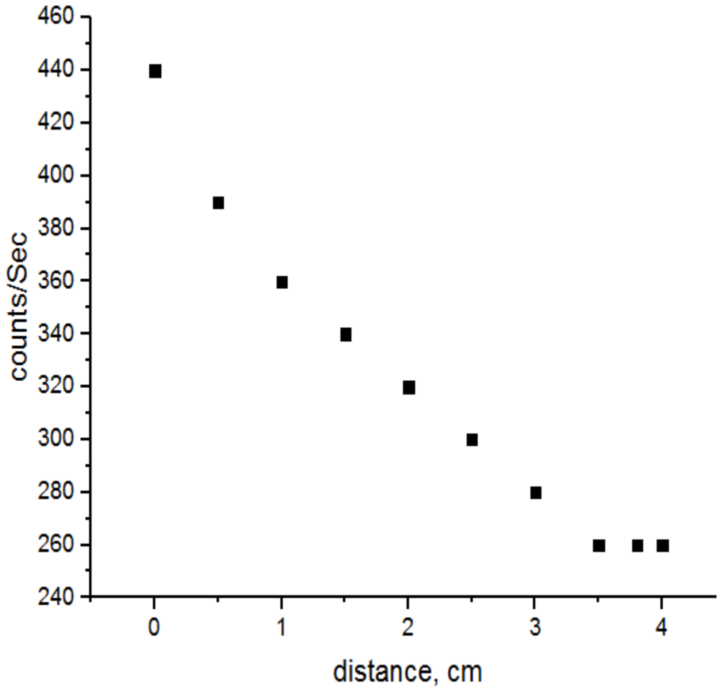

# *Pixel Detector*

## *task 6*

Prepared by:

**Alaa ElSadieque**

# Introduction

- The notion of pixel (short for "picture element") has been introduced in image processing to describe the smallest discernable element in a given process or device.
- A pixel detector is a device able to detect an image and the size of the pixel corresponds to the granularity of the image. The omnipresent digital cameras are a typical example of pixel detectors. In this case, photons of different energies are integrated in the sensing elements (pixel) during a short exposure time and generate an intensity distribution which is the image.

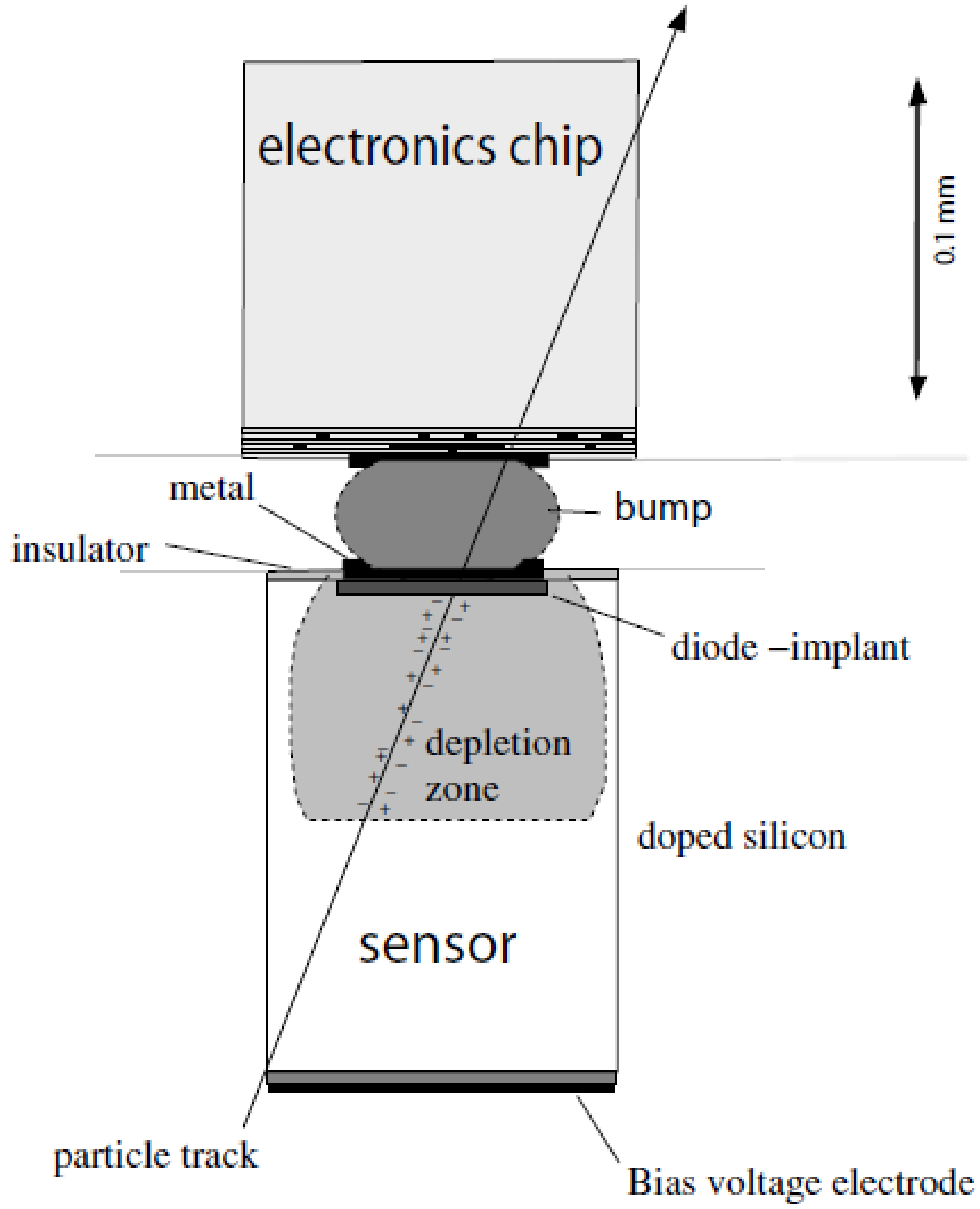
electronics chip
0.1 mm
metal
bump
insulator
diode –implant
depletion
zone
doped silicon
sensor
particle track
Bias voltage electrode

- this Schematic view of one pixel cell, the basic building block of a hybrid pixel detector. The ionizing particle crosses the sensor and generates charges that, moving in the depletion region under the action of an electric field, produce signals.These are amplified, and hit pixels are identified and stored by the electronics. The thickness of the sensitive part of the detector – the depletion zone – depends on the bias voltage and on the sensor parameters.

# Evolution of Pixel Detectors in Particle Physics

- The birth of pixel detectors can be traced back to the 1984 IEEE Nuclear Science Symposium where Gaalema pointed out that an integrated circuit for focal plane imaging sensors, developed by Hughes Aircraft Co., could be connected, through bump bonding, to a semiconductor diode array to detect and localize X-rays.

- The first pixel matrix, OmegaD(The heavy ion experiments using the CERN Omega spectrometer were the first to use pixel detectors) had 1,024 pixels of size 75 × 500 µm2 (16 columns and 64 rows). The readout chip, connected to the mating sensor through solder bumps was realized in CMOS technology. Each channel had a continuously sensitive preamplifier followed by an asynchronous comparator and a digital delay line through which the discriminated signals travel waiting for an external trigger. When the trigger is received all pixels with a coincident delay line signal are read out

- The power dissipation was 30 μW per pixel (i.e. ≈1mW/mm2); the electronics noise was just below 100 e− rms while the threshold variation between channels was around 500 e− rms. This last number dominates the noise of the chip even if it is not an intrinsic noise contribution.
- This observation already points to a problem: one individual pixel circuit can have excellent performance, but it is difficult to get by design a correspondingly good response uniformity over the whole chip area. Both technological limitations (e.g. electronics parameter variations over the chip area) and design choices (e.g. sensitivity to voltage drops along busses) contribute to nonuniformities. These sources of fluctuations cannot be completely eliminated and modern front-end chips dedicate part of the pixel cell area to trimming circuits. This became possible with the adoption of deep submicron (DSM) technologies featuring 0.25-μm structure sizes, while it was not practical in the 3 μm technology used for the OmegaD chip.

- Several generations of pixel chips have been necessary to evolve from OmegaD to ALICE1. The intermediate chips, intensively used in heavy ion experiments, have allowed one to gain considerable experience on system aspects.

- Moving from a “proof of principle,” where 3 single-chip detectors have to operate for some hours close to a beam, to a system made of 84 multichip detectors to be used in experiments lasting months requires one to solve new problems. In general, there is the need to keep the detector specifications stable during production through the control of the critical fabrication processes and during the experiment through the control of the critical environmental and operational parameters. This was done for the experiment WA97 where a telescope of seven pixel planes, each having 72,576 pixels and covering ≈29 cm2

- Over the last four decades, experimental particle physics progressively moved from fixed target to colliding beam accelerators as these bring several advantages, the most relevant being the significantly higher energy that can be reached in the collision between elementary particles. Particles produced in a colliding beam accelerator are spread out over a very large solid angle, which has then to be covered by large area detectors.
- Space resolution, granularity, and radiation resistance make pixel detectors ideal as vertex detectors and they must therefore be the first device encountered by the particles emerging from the interactions. Since the information carried by particles is deteriorated when passing through matter, minimal material has to be used to support and operate pixel detectors around a colliding beam accelerator.

# Applications

- Even if the pixel detectors were born for the needs of particle physics, they are potentially very useful in other domains where fast imaging with penetrating radiation is necessary.
- Some applications in medicine, biology, and astrophysics is needed. Their success will greatly depend on the cost per square centimeter of detector. This is presently quite high (≈e500), but can be sensibly reduced if large-scale applications could be envisaged and if some of the special requirements needed for particle physics applications (e.g. tens of kilogray radiation hardness) could be dropped. The high-density connectivity is a critical and expensive production step that is typical of the hybrid pixel design and not very much used in other applications. Some new pixel developmentstry to avoid this step joining more intimately sensors and electronics. This also means compromises in performances, but may simplify the production steps and finally open the door to a still wider range of applications.

# Refernces

1. L.Rossi, P.Fischer, T .Rohe, NWermes. Pixel detectors: From fundamentals to applications. Springer Science & Business Media; 2006 Jan 18.
2. J. Millaud, M. Wright, D. Nygren: A pixel unit cell targeting 16 ns resolution and radiation hardness in a column read-out particle vertex detector. Report LBL-32912 (1992).
3. J. Ulrici et al: Nucl. Instrum. Methods A **547**, 424–436 (2005)